Temperature measurement using frequency comb absorption spectroscopy of CO2

Hänsel, Andreas; Reyes Reyes, Adonis; Persijn, ST; Urbach, Paul; Bhattacharya, Nandini

DOI
10.1063/1.4984252

Publication date
2017

Document Version
Final published version

Published in
Review of Scientific Instruments

Temperature measurement using frequency comb absorption spectroscopy of CO_2

A. Hänsel, A. Reyes-Reyes, S. T. Persijn, H. P. Urbach, and N. Bhattacharya

Citation: Review of Scientific Instruments **88**, 053113 (2017);
View online: https://doi.org/10.1063/1.4984252
View Table of Contents: http://aip.scitation.org/toc/rsi/88/5
Published by the American Institute of Physics

REVIEW OF SCIENTIFIC INSTRUMENTS **88**, 053113 (2017)

Temperature measurement using frequency comb absorption spectroscopy of CO_2

A. Hänsel,[1,a)] A. Reyes-Reyes,[1] S. T. Persijn,[2] H. P. Urbach,[1] and N. Bhattacharya[1,b)]
[1]*Department of Imaging Physics, Faculty of Applied Sciences, University of Technology, Lorentzweg 1, 2628 CJ Delft, The Netherlands*
[2]*VSL, Dutch Metrology Institute, Thijsseweg 11, 2629 JA Delft, The Netherlands*

(Received 30 November 2016; accepted 15 May 2017; published online 31 May 2017)

Absorption spectroscopy on CO_2 for the determination of gas temperature is reported. Direct absorption of a frequency comb laser through a gas cell at atmospheric conditions is analysed with a virtually imaged phased array spectrometer. Several measurement and analysis techniques are investigated to find the parameters most sensitive to changes in the temperature. Some of these show qualitative agreement with theoretical predictions where the trend is similar to the calculated values. *Published by AIP Publishing.* [http://dx.doi.org/10.1063/1.4984252]

I. INTRODUCTION

It is the goal of spectroscopy to gather knowledge about a material, e.g., a gas sample, by probing it with electromagnetic waves. The applications for this research are manifold. Human breath analysis allows for non-invasive testing for diseases.[1–3] Climate-relevant atmospheric gases can be monitored to improve current models and predict climate changes.[4] Spectroscopy also provides insights into the structure of matter. With the advent of lasers in 1960, this field showed remarkable progress, allowing the measurement of spectral lines with unprecedented accuracy. Prior to the invention of the laser, spectroscopy was implemented with broadband illumination and interrogation with a spectrometer. Spectrometers included Michelson interferometer, Fabry-Perot interferometers, grating spectrometers, and many more. They used interference of light waves to create a wavelength selective transmission, either in amplitude, such as in the Michelson interferometer, or in propagation direction, such as in the case of the grating. Prism spectrometers, on the other hand, were exploiting the dispersion of light in a medium. Interference-based spectrometers had to be designed around the trade off between resolution and ambiguity range, expressed by the free spectral range (FSR). The emergence of tunable coherent sources, like tunable single mode diode lasers, was a milestone in spectroscopic measurements as they allowed for absorption measurements that can be both, of high resolution and yet cover a broad wavelength range.[5] Such a setup requires a tunable single mode laser and a broadband detector. The wavelength range needs to be scanned and the spectrum cannot be obtained in a single shot. Due to the intrinsic coherence of single mode laser systems, this approach allowed for long propagation ranges as well as high frequency resolution. Using classical broadband light sources, such as diodes or candescent light sources, for long distance measurements proves to be more difficult, as an increase in bandwidth reduces the coherence time of the light. In addition to temporal coherence, spatial coherence needs to be considered. Such light sources can be broadband, but the limited temporal and spatial coherence is restrictive for long distance measurements, where beam collimation needs to be controlled accurately. The development of the frequency comb remedied this situation,[6–8] providing a broadband and yet coherent light source. In a frequency comb, multiple narrow linewidth laser lines are present, creating a comb structure in the spectral domain. As a consequence, the coherence function shows a periodicity governed by the repetition frequency with a slowly falling envelope, which depends on the noise in the laser system.[9] A frequency comb therefore has the ability to probe many wavelengths simultaneously with the long coherence length of individual single mode lasers.[10] The advantages and disadvantages are discussed in several publications.[11,12]

Apart from spectroscopic studies, frequency combs and single mode lasers have been used for long distance measurements. If those measurements are not taken in vacuum but atmospheric air, the variations of the refractive index of air limit the precision of the measurement.[13–18] To reach uncertainties in the 10^{-7} regime, temperatures need to be known with accuracies of ~100 mK.[19] Modern highly accurate long distance measurements are at these limits. State of the art measurements reached relative accuracies of 10^{-7} and 10^{-8} in air using single mode lasers and frequency combs, respectively.[20–25] Two colour schemes to compensate for refractive index uncertainty were also applied.[26] Edlén provided a tool to determine the refractive index of air if its composition, pressure, and temperature are known.[27] Since then Edlén's equation has been continuously updated and modified.[28–30]

Among the parameters pressure, composition, and temperature, the latter shows the strongest local variations, whereas the other two remain constant over a relatively large area.[31] Therefore, several temperature sensors are commonly placed along the beam path. Classical thermometers are localised in nature and can be based, e.g., on the density

a)Electronic mail: A.Hansel@tudelft.nl
b)Electronic mail: N.Bhattacharya@tudelft.nl

of a liquid, expansion of a solid, the change of thermal radiation, or changes in the electrical conductivity. All of these measurements share the property that the data are obtained at a single point in space. Retrieving line or volumetric data requires placing a whole array of detectors in or close to the region of interest. If the environmental parameters could be obtained spectroscopically and the same laser beam be used for the distance measurements, the experiment would be more efficient and accurate. Instead of measuring the temperature along the beam it can be measured exactly at the propagation path. Temperatures measured this way will automatically be integrated line data, as each point in the propagation path of the beam provides data. Distance measurements based on interferometry read out the phase necessitating the use of the absorption of the medium propagated through to determine the temperature. Suitable candidates are O_2 and CO_2, since both show absorption lines in the accessible wavelength range of visible light and near infra-red.[32] O_2 has a larger abundance in air and shows absorption in the visible wavelength range. State of the art measurements reach accuracies of 7 mK using a diode-laser-based setup, as reported by Hieta *et al.*[33] A recent publication by the same group showed the feasibility of using this method for outdoor temperature measurements.[34] Fiber-based sources show the advantage of stability towards ambient changes and portability and are preferred sources for outdoor measurements. However, to access the relevant visible lines for O_2 spectroscopy with fiber-based frequency combs, second harmonic generation (SHG) or other wavelength conversion methods have to be used, since it lies outside of the coverable wavelength range of such a laser source. Ti:Saph oscillator based frequency combs reach visible wavelengths but show, due to the lack of integration, limited performance if a portable setup is required. CO_2, on the other hand, shows strong absorption in the emission range of Erbium doped fiber lasers, such as the one used in this study. Those laser sources can be completely integrated and can be relatively independent of the measurement environment. As a consequence, they are great candidates for a portable setup. CO_2 temperature measurements have already been reported by Farooq *et al.* using diode laser absorption measurements at 2.7 μm wavelength.[35] These experiments have been conducted for the high temperatures of combustion gasses, which are outside of what is reachable with even extreme weather conditions. Recent publications show an interest to expand spectroscopic temperature measurements in CO_2 to lower temperatures.[36] For climate research, several applications focus on identifying the concentration of CO_2 in air; the techniques used there can be used for temperature determination assuming the concentration of CO_2 can be retrieved on a different channel. Spectroscopic measurements with propagation lengths of 2 km have already been reported.[4] Care has to be taken to select CO_2 absorption lines that are not overlapping with those of water. The water content in air is another quantity which can show strong local variations.

In this work, we report temperature measurements of CO_2 in a gas cell. Due to its low concentration in the atmosphere, first feasibility investigations of CO_2 were conducted in a controlled atmosphere.

II. METHOD

The optical absorption of a gas reveals information about the constituents of the gas. This is used in spectroscopy to identify and quantify gases but can also be used to determine the temperature and pressure of the gas mixture, if the gas composition is known. We investigated the temperature dependence of pure CO_2 absorption in the near infra-red region (NIR), while keeping pressure and gas concentration fixed. The strength of an absorption line depends on the population densities of lower and upper states involved in the line transition and the number of absorbers, i.e., molecules, exposed to the light. Interactions between absorbers can lead to effects like line broadening beyond the natural linewidth. An increase in the absorption linewidth corresponds to a decrease in the maximum absorption, while the total area under the absorption curve remains the same, which is the case when changing the pressure, but keeping temperature and number of absorbing molecules constant. Therefore, we compare these areas for different samples. Besides the temperature dependence given by the Boltzmann distribution of the population densities, a temperature change influences the amount of absorbers in a given volume when keeping the pressure constant. Both effects are expected to lead to an impact on the absorption measurements.[33] Evaluating absorption lines in the HITRAN database shows that the temperature dependence is rather weak, leading to requirements for a very accurate spectroscopic setup to be able to monitor corresponding absorption profile changes.[32]

In this setup, we will take absorption spectra at two different temperatures and compare the differences in peak area and height of several absorption lines (simple integration as well as line fitting). Other publications[33,34] gave reasons for measuring line ratios instead requiring a more complex data treatment. The absorber number density needs to be determined requiring accurate measurements of pressure and distance. A separate calculation for this quantity can be omitted here, as its effect can be part of the calibration. The comparison of directly measurable quantities simplifies the noise determination, which motivated the analysis presented here. To compare measurement to simulation, we will show whether the measured changes are in line with what is predicted by the HITRAN database.

III. EXPERIMENTAL SETUP

The setup consists of three main components, namely the laser source, the interaction cell, and the detector. Single mode fibers (Thorlabs P1-SMF28E-FC) are used to guide the light between the general components. The setup is shown in Fig. 1.

The laser source is an Erbium doped fiber frequency comb laser with a repetition rate of 100 MHz from Toptica and emits light in the wavelength range of 1400–1600 nm. A highly nonlinear fiber (HNF) was required to reach the spectral lines that were measured in this work. To guide the light to the gas cell it is coupled into a single mode fiber.

The gas cell has a length of 1.5 m and a volume of 480 ml. It can be filled with CO_2, N_2, or be evacuated. The gas flow is

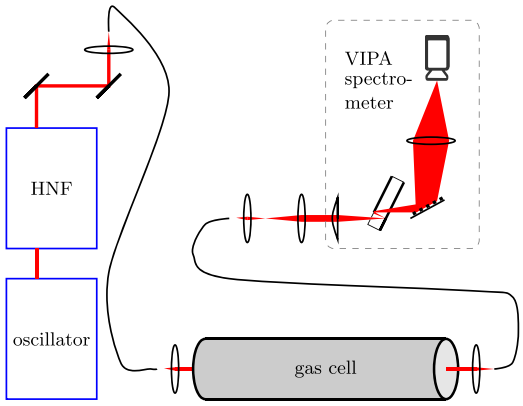

FIG. 1. The highly nonlinear fiber (HNF) broadens the spectrum to wavelength regions that are not covered by the laser oscillator. The fibers serve as apertures and simplify guidance of the beam between the laser output, gas cell, and spectrometer. Not shown in the setup are heating wires coiled around, the thermometer placed inside the gas cell as well as the gas flow equipment, also attached to the gas cell.

controlled with mass flow controllers (Bronkhorst F-201CV-1K0-RAD-22-V) at the entrance side and a pressure controller (P-702CV-1K1A-RAD-22-V) at the exit side. The pressure controller is connected to a Vacuubrand MD 1 vacuum pump. To be able to increase the temperature, a heating wire has been wrapped around the gas cell. A temperature sensor (Pico Technology PT-104 with an SE012 Pt100 probe) is placed in the gas cell to monitor the temperature in the cell. These devices are not included in Fig. 1.

The virtually imaged phased array (VIPA) spectrometer[37] is made in house and consists of the VIPA etalon from Precision Photonics (S-LAA71), a grating as post-disperser (Spectrogon UK, G1100 31 50 10 NIR, 1100 lines/mm) and an infra-red camera (XenICs XEVAFPA-1.7-640) as well as two lenses, one of them cylindrical as can be seen in Figs. 1 and 2. For lenses, mirrors, and fiber incouplers, readily available components from Thorlabs have been used.

A. VIPA spectrometer

A Virtually Imaged Phased Array (VIPA) spectrometer has been used to record the spectra.[37] In a VIPA multiple virtual sources interfere and create a wavelength dependent transmission for certain direction. Similar to a grating, it acts as an angular disperser separating wavelengths by different propagation angles. Virtual sources are created by focussing the laser beam at the backplane of the VIPA etalon. The etalon

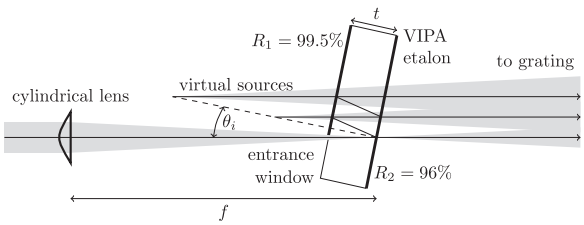

FIG. 2. A focussed spot at the backplane mirror creates multiple virtual sources leading to a wavelength selective transmission for different propagation angles. Reproduced with permission from Rev. Sci. Instrum. **87**, 093107 (2016). Copyright 2016 AIP Publishing LLC.[43]

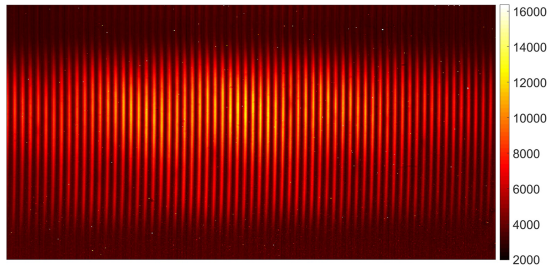

FIG. 3. Typical VIPA spectrometer image. When stitching together neighbouring modes spectral line data can be read out. The image shows the power per pixel in arbitrary units. The images taken have 640 × 512 pixels. The FSR corresponds to 400 pixels, corresponding to 125 MHz per pixel. In comparison: the resolution of the spectrometer is 680 MHz.

consists of a glass plate with reflective coatings at the entrance side ($R_1 = 99.5\%$) and the output side ($R_2 = 96\%$). Reflections from those two interfaces create the new point sources consisting of virtual images of the focussed beam. If a cylindrical lens is used, a grating can be used as a post-disperser eliminating the drawback of the low free spectral range (FSR). The FSR of the VIPA spectrometer depends on the thickness t, refractive index n_g of the glass plate, and the incidence angle θ_i of the focussed laser beam. Very low incidence angles are common ($\theta_i \approx 0$), such that the FSR can be approximated by FSR $\approx \frac{c}{2n_g t}$, which is 50 GHz in our spectrometer. A lens after the grating will image different propagation angles to different positions on the camera. Spectral data are contained in adjacent lines representing one FSR of 50 GHz each. The resolution of the spectrometer is 680 MHz. A typical image produced by such a spectrometer is shown in Fig. 3. By stitching together spectral data from neighbouring lines, a full spectrum is obtained. In order to perform the stitching procedure, the pixel representation of the free spectral range on the camera needs to be identified. This can be done by illumination with a single mode laser source (Roithner LaserTechnik SPL1430-2-9-PD) or if a clear repeating pattern can be identified by directly looking at the camera image. The full integration with fibers allows for easy replacement of the source and spectrometer. In this setup, the free spectral range was directly determined from the measured camera image and later confirmed with the single mode laser. If the frequency comb modes can be resolved a more accurate frequency calibration is possible.[38]

IV. MEASUREMENT PROCEDURE

For a typical measurement, the gas cell is filled with pure CO_2 at a pressure of 1 atm at room temperature. The pressure is controlled with a pressure controller while a steady flow is applied. For filling, the cell flow speeds of 1000 ml_n/min for N_2 and 500 ml_n/min for CO_2 were applied. When the gas cell was filled completely, it was lowered to 10 ml_n/min to keep a steady flow. The spectrum is measured using the VIPA spectrometer. Subsequently a reference image needs to be taken either by evacuating the cavity or by flushing it with N_2, which does not show absorption at the measured wavelength range. Both methods show identical results at room temperature. At higher temperatures, however, the latter one performs better, showing

more consistent absorption changes. To increase the temperature, a heating wire, which is coiled around the gas cell, is used. Once the temperature reaches equilibrium at the higher temperature, the aforementioned routine can be applied again. A dark image needs to be subtracted to minimise the error introduced by the camera. For the same reason, an averaging procedure was applied to the camera images. Two hundred averages were used for these measurements. The measured temperature differences ranged up to 10 K, which is shown in Fig. 7.

The measurements at room temperature can be done in a few minutes, as only the filling/evacuation of the gas cell takes a significant time. The measurements at higher temperature need longer, i.e., several hours, due to the time it takes the temperature of the inserted gas to reach a steady state.

V. RESULTS

For this study, CO_2 lines between 6915 and 6975 cm^{-1} were used, which correspond to the wavelengths around 1.44 μm. The investigation included 22 different lines whose labelling can be found in Fig. 4. The lines of (P44, P42,. . . , P2) are corresponding to the line numbers (1, 2,. . . , 22) in the nomenclature of this publication. In Fig. 5, the predicted change in peak height from HITRAN can be seen when increasing the temperature. An increase by 5 K results in a change of less than one percent, placing very stringent constraints on the measurements.

Several parameters were compared to determine the most suitable one for temperature measurements among which are peak height, integrated peak area as well as fitted line profile area. For the peak height, the highest reached absorption value per peak was read out. For integrating the peak area, the interval was chosen to minimise the influence of neighbour peaks limiting the integration window to each of the investigated lines. This meant integrating between the two neighbouring minima of the peak. Fitted line area is expected to provide better results. For fitting and peak analysis, Origin has been used.[39] A Lorentzian fit to measured data can be found in Fig. 6. An

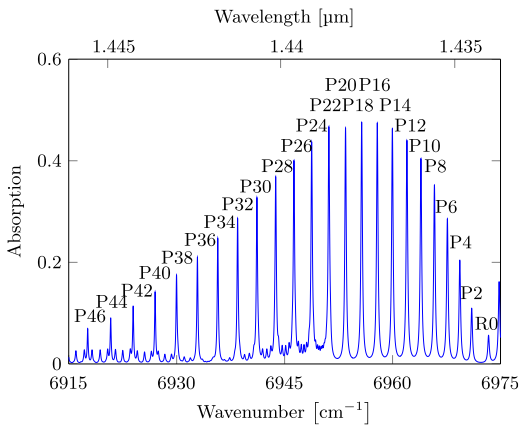

FIG. 4. Nomenclature of the investigated CO_2 absorption lines in the 3 ν_3 band[41] as labelled in HITRAN. The shown absorption profile corresponds to 1.5 m of propagation through pure CO_2 at the pressure of 1 atm and a temperature of 296 K.

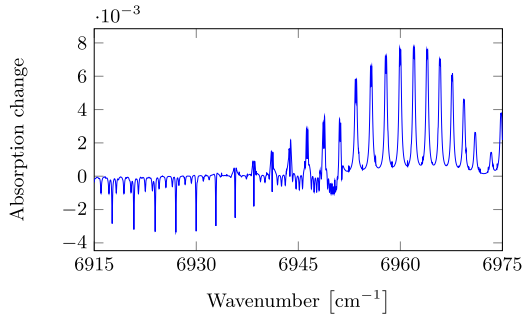

FIG. 5. Expected change when increasing the temperature of pure CO_2 by 5 K. The plot shows the absolute difference in absorption [A(T = 296 K)−A(T = 301 K)] for propagation through 1.5 m pure CO_2 at a pressure of 1 atm. The strength of the corresponding absorption lines is shown in Fig. 4.

alternative line shape is the Voigt profile, which is a convolution of Gaussian and Lorentzian line shape. In the investigated regime, the Lorentzian contribution is dominant. The fitting algorithm showed better convergence and led to smaller fitting error estimates, which is why the Lorentzian profile was used. The parameters were calculated for the HITRAN data and the measured data to evaluate whether their performance was similar. Figure 7 shows the change in linestrength for each of the 22 individual lines that have been investigated. As can be seen, HITRAN and measurement show substantial deviations.

At higher temperatures, the beam shows increased divergence. In consequence, the focus position of the fiber incoupler deviates from its original position, resulting in a decreasing coupling efficiency and hence a drop of the transmission baseline.[40] When taking vacuum reference images, measurement and reference beams experience a different beam divergence. N_2 reference images share the beam divergence with the CO_2 measurement and, since the ratio of the intensities of both beams is used to obtain the spectrum, in theory can assume an unchanged transmission baseline level, despite being at lower signal level. Nitrogen can be introduced by refilling an

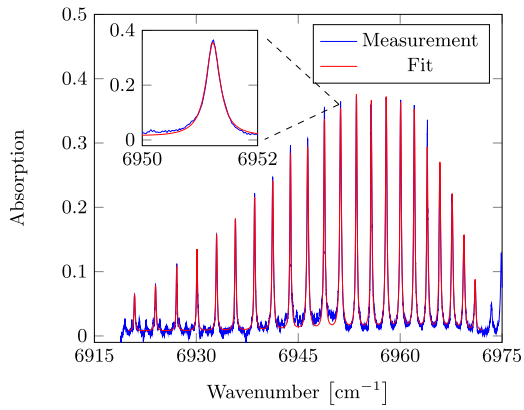

FIG. 6. Multi-line Lorentzian fit to the measured spectrum at 26.9 °C. The fit is displayed in red, while the measured data are shown in blue. The variation of the baseline as well as the presence of weak lines in the vicinity of the main absorption peaks leads to difficulties in the fitting procedure. Only the main absorption lines were included as fitting parameters. The inset is zooming in on line number 12. The measurement shows a good qualitative agreement with the HITRAN data (Fig. 4). Comparing the peak heights of measurement and HITRAN shows a disagreement of 20%. Possible explanations for this include instrumental spread of the spectrometer as well as nonlinearity of the camera.

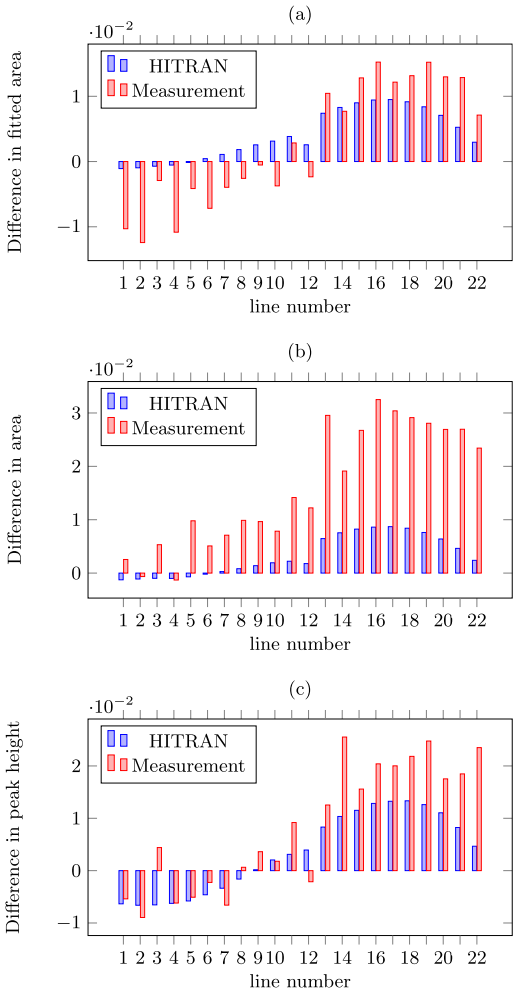

FIG. 7. Changes in absorption for the different investigated absorption lines when increasing the temperature by ≈10 K (from 26.9 °C to 36.7 °C). The beam propagated through 1.5 m of pure CO_2 at a pressure of 1 atm. The reference image was taken by flushing the cell with N_2. (a) Comparison of the area under the curve when fitting a multi-line Lorentzian profile. The measured temperature would be interpreted to be 5 K higher than the read-out from HITRAN, with an estimated uncertainty of 3 K. (b) Comparison when the lines are simply integrated without assuming any line shape. In (c) only the peak height was compared. The measurement (shown in red) generally shows a stronger reaction to the temperature changes than HITRAN data (blue).

evacuated gas cell or by continuously flushing it into the gas cell. The downside of the latter method is that more nitrogen needs to be introduced to ensure that no carbon dioxide is remaining in the gas cell. This is also advantageous since the pressure in the gas cell does not change and the gas cell windows remain steady. Any baseline level change is compensated by scaling the transmission profile accordingly but introduces an additional error, which is more prominent in the case where a vacuum reference image is taken. Both methods, vacuum and N_2 as reference, have been investigated with the latter showing better performance. The results with the N_2 reference are shown in Fig. 7. As expected the simple integration of the line area leads to stronger deviations than the fitted area.

Camera noise posed another difficulty since several pixels were malfunctioning and had to be excluded from the data analysis further reducing the quality of the obtainable spectrum. Less than one percent of the pixels had to be excluded, which should not affect the fitting severely. Camera noise is about two percent of the intensity maximum after removal of the dark image and excluding dead pixels. The intensity range is reduced when the baseline signal is reduced, which effectively amplifies the camera noise by the factor $(I_{\text{full}} - I_{\text{dark}})/(I_{\text{reduced}} - I_{\text{dark}})$, which is up to factor two in our measurements. Since the noise is present in measurement and reference image, the contribution of the noise is effectively doubled when creating the line spectrum. The camera showed strong nonlinearities at high power levels close to saturation as well as at low power levels. With the removal of dark noise, the contributions at low power levels are not critical. A limited number of pixels reached power levels where the saturation effects can affect the data. The measured peak absorption is underestimated up to 20% due to camera nonlinearities. This is due to the reference image having a higher power level than expressed by the camera in certain parts of the spectrum. The corresponding error contribution on the fitting procedure cannot be easily predicted, as not all the pixels are affected. While the measured data and HITRAN show a similar trend, there are quantitative differences which make a comparison with simulated data difficult. It is advisable to reduce the amount of lines taken into account for the temperature determination to the strongest lines, e.g., the lines 14–20, which show the best overlap between measured data and HITRAN. Additionally lines that are at the stitching points when generating line data out of the 2D image should be excluded, as the line shape is strongly disturbed. With this reduced set of lines, the absorption changes for Lorentzian line profile fits are ≈50% higher in the case of measured data when compared to HITRAN. For the investigated temperature change of 10 K, this results in a deviation of 5 K. As can be seen from Fig. 7, the absorption changes show a regular pattern for HITRAN data, whereas the measured values fluctuate. The standard deviation is approximately 30%, here 3 K. Increasing the data set might be able to reduce this number. The errors are significantly higher in the case of line integration, without fitting and peak height comparison. The uncertainty of the reported line strength in HITRAN is listed as ≥1% and <2% for the investigated lines. In consequence, the error listed from the database is higher than the effect to be measured, which clearly suggests an independent calibration of the method.

VI. CONCLUSION

We report a temperature measurement in a CO_2 filled gas cell using a frequency comb laser and a VIPA spectrometer. Spectroscopic measurements with the compact robust frequency combs in the 1.5 μm range make CO_2 a possible candidate for the temperature determination of ambient air. The main challenges for using CO_2 are as follows: finding absorption windows free of H_2O absorption, finding lines which show sufficient sensitivity to temperature, and obtaining well separated absorption lines which have low background absorption from other sources and a stable concentration. To test the feasibility, measurements were carried out using different protocols for the reference measurement. For this, an evacuated cell and a N_2 filled cell were used alternatively.

We found that the N_2 filled cell provided a better reference. Analysis of the absorption spectra was also carried out with the view to observe variations in the parameters like peak height, area under the absorption line, and absorption profile fitting of the spectral lines. The best fits were obtained with the Lorentzian line shape which dominates the regime of our measurement with respect to parameters like pressure and flow in our experimental setup. The major disruptive factors to this method were the power loss with increased temperature and camera noise, but these issues will also have to be encountered if the method is to be further developed for field measurements. At this stage, the comparison with HITRAN shows a qualitative overlap. Further engineering and optimisation of the measurement is required for quantitative comparisons. The technique presented here can be very useful in non-contact temperature measurements in case of hazardous environments and for remote monitoring besides the obvious advantage to long distance measurements. It can be combined with metrologic measurements that read out the phase, as only the absorption of the CO_2 is required for the temperature determination. The temperature dependent changes in the absorption lines when calibrated with *a priori* measurement can also be used for temperature monitoring. For certain applications, the presented method can be improved by combining it with optical cavities or optical waveguides to increase the interaction between light and air.[38,42] This, however, would prevent the usability for long distance measurements.

ACKNOWLEDGMENTS

This work was funded through the European Metrology Research Program (EMRP), Project No. SIB60 Surveying and the Dutch Ministry of Economic Affairs. The EMRP is jointly funded by the EMRP participating countries within EURAMET and the European Union.

[1]M. J. Thorpe, D. Balslev-Clausen, M. S. Kirchner, and J. Ye, "Cavity-enhanced optical frequency comb spectroscopy: Application to human breath analysis," Opt. Express **16**, 2387–2397 (2008).
[2]E. van Mastrigt, A. Reyes-Reyes, K. Brand, N. Bhattacharya, H. P. Urbach, A. P. Stubbs, J. C. de Jongste, and M. W. Pijnenburg, "Exhaled breath profiling using broadband quantum cascade laser-based spectroscopy in healthy children and children with asthma and cystic fibrosis," J. Breath Res. **10**, 026003 (2016).
[3]M. R. McCurdy, Y. Bakhirkin, G. Wysocki, R. Lewicki, and F. K. Tittel, "Recent advances of laser-spectroscopy-based techniques for applications in breath analysis," J. Breath Res. **1**, 014001 (2007).
[4]G. B. Rieker, F. R. Giorgetta, W. C. Swann, J. Kofler, A. M. Zolot, L. C. Sinclair, E. Baumann, C. Cromer, G. Petron, C. Sweeney, P. P. Tans, I. Coddington, and N. R. Newbury, "Frequency-comb-based remote sensing of greenhouse gases over kilometer air paths," Optica **1**, 290–298 (2014).
[5]P. Werle, "A review of recent advances in semiconductor laser based gas monitors," Spectrochim. Acta, Part A **54**, 197–236 (1998).
[6]T. W. Hänsch, "Nobel lecture: Passion for precision," Rev. Mod. Phys. **78**, 1297–1309 (2006).
[7]J. L. Hall, "Nobel lecture: Defining and measuring optical frequencies," Rev. Mod. Phys. **78**, 1279–1295 (2006).
[8]S. A. Diddams, "The evolving optical frequency comb [Invited]," J. Opt. Soc. Am. B **27**(11), B51–B62 (2010).
[9]R. Paschotta, A. Schlatter, S. C. Zeller, H. R. Telle, and U. Keller, "Optical phase noise and carrier-envelope offset noise of mode-locked lasers," Appl. Phys. B **82**, 265–273 (2006).
[10]S. A. Diddams, L. Hollberg, and V. Mbele, "Molecular fingerprinting with the resolved modes of a femtosecond laser frequency comb," Nature **445**, 627–630 (2007).
[11]M. C. Stowe, M. J. Thorpe, A. Pe'er, J. Ye, J. E. Stalnaker, V. Gerginov, and S. A. Diddams, "Direct frequency comb spectroscopy," Adv. At., Mol., Opt. Phys. **55**, 1–60 (2008).
[12]D. Felinto and J. Ye, "Direct frequency comb spectroscopy," in *Latin America Optics and Photonics Conference, OSA Technical Digest (CD)* (Optical Society of America, 2010), paper WG2.
[13]J. Ye, "Absolute measurement of a long, arbitrary distance to less than an optical fringe," Opt. Lett. **29**(10), 1153–1155 (2004).
[14]M. Cui, M. G. Zeitouny, N. Bhattacharya, S. A. van den Berg, H. P. Urbach, and J. J. M. Braat, "High-accuracy long-distance measurements in air with a frequency comb laser," Opt. Lett. **34**(13), 1982–1984 (2009).
[15]M. Cui, M. G. Zeitouny, N. Bhattacharya, S. A. van den Berg, and H. P. Urbach, "Long distance measurement with femtosecond pulses using a dispersive interferometer," Opt. Express **19**, 6549–6562 (2011).
[16]J. Lee, Y.-J. Kim, K. Lee, S. Lee, and S.-W. Kim, "Time-of-flight measurement with femtosecond light pulses," Nat. Photonics **4**, 716–720 (2010).
[17]K.-N. Joo and S.-W. Kim, "Absolute distance measurement by dispersive interferometry using a femtosecond pulse laser," Opt. Express **14**, 5954–5960 (2006).
[18]K. Minoshima and H. Matsumoto, "High-accuracy measurement of 240-m distance in an optical tunnel by use of a compact femtosecond laser," Appl. Opt. **39**, 5512–5517 (2000).
[19]T. Hieta and M. Merimaa, "Spectroscopic measurement of air temperature," Int. J. Thermophys. **31**, 1710–1718 (2010).
[20]J. Guillory, R. Šmíd, J. García-Márquez, D. Truong, C. Alexandre, and J.-P. Wallerand, "High resolution kilometric range optical telemetry in air by radio frequency phase measurement," Rev. Sci. Instrum. **87**, 075105 (2016).
[21]J. Guillory, J.-P. Wallerand, A. F. Obaton, and C. Alexandre, "Laser diodes based absolute distance meter," in *Conference on Precision Electromagnetic Measurements (CPEM)* (IEEE, Rio de Janeiro, 2014), pp. 490–491.
[22]I. Coddington, W. C. Swann, L. Nenadovic, and N. R. Newbury, "Rapid and precise absolute distance measurements at long range," Nat. Photonics **3**, 351–356 (2009).
[23]S. A. van den Berg, S. T. Persijn, G. J. P. Kok, M. G. Zeitouny, and N. Bhattacharya, "Many-wavelength interferometry with thousands of lasers for absolute distance measurement," Phys. Rev. Lett. **108**, 183901 (2012).
[24]S. A. van den Berg, S. van Eldik, and N. Bhattacharya, "Mode-resolved frequency comb interferometry for high-accuracy long distance measurement," Sci. Rep. **5**, 14661 (2015).
[25]N. R. Doloca, K. Meiners-Hagen, M. Wedde, F. Pollinger, and A. Abou-Zeid, "Absolute distance measurement system using a femtosecond laser as a modulator," Meas. Sci. Technol. **21**, 115302 (2010).
[26]K. Minoshima, K. Arai, and H. Inaba, "High-accuracy self-correction of refractive index of air using two-color interferometry of optical frequency combs," Opt. Express **19**, 26095–26105 (2011).
[27]B. Edlén, "The dispersion of standard air," J. Opt. Soc. Am. **43**, 339–344 (1953).
[28]B. Edlén, "The refractive index of air," Metrologia **2**, 71–80 (1965).
[29]P. E. Ciddor, "Refractive index of air: New equations for the visible and near infrared," Appl. Opt. **35**, 1566–1573 (1996).
[30]G. Bönsch and E. Potulski, "Measurement of the refractive index of air and comparison with modified Edlén's formulae," Metrologia **35**, 133–139 (1998).
[31]R. B. Stull, *An Introduction to Boundary Layer Meteorology* (Kluwer Academic Publishers, 1988).
[32]See http://hitran.iao.ru/ for HITRAN on the web (accessed Oct. 17 2016).
[33]T. Hieta, M. Merimaa, M. Vainio, J. Seppä, and A. Lassila, "High-precision diode-laser-based temperature measurement for air refractive index compensation," Appl. Opt. **50**, 5990–5998 (2011).
[34]T. Tomberg, T. Fordell, J. Jokela, M. Merimaa, and T. Hieta, "Spectroscopic thermometry for long distance surveying," Appl. Opt. **56**, 239–246 (2017).
[35]A. Farooq, J. Jeffries, and R. Hanson, "CO_2 concentration and temperature sensor for combustion gases using diode-laser absorption near 2.7 μm," Appl. Phys. B **90**, 619–628 (2008).

[36]A. Klose, G. Ycas, F. C. Cruz, D. L. Maser, and S. A. Diddams, "Rapid, broadband spectroscopic temperature measurement of CO_2 using VIPA spectroscopy," Appl. Phys. B **122**, 78 (2016).
[37]S. Xiao and A. Weiner, "2-D wavelength demultiplexer with potential for ≥1000 channels in the C-band," Opt. Express **12**, 2895–2902 (2004).
[38]G. Kowzan, K. F. Lee, M. Paradowska, M. Borkowski, P. Ablewski, S. Wójtewicz, K. Stec, D. Lisak, M. E. Fermann, R. S. Trawiński, and P. Masłowski, "Self-referenced, accurate and sensitive optical frequency comb spectroscopy with a virtually imaged phased array spectrometer," Opt. Lett. **41**, 974–977 (2016).
[39]See http://originlab.com/ for Origin Pro 2015.
[40]L. C. Andrews and R. L. Phillips, *Laser Beam Propagation through Random Media* (SPIE Press, 2005).
[41]R. A. Toth, R. H. Hunt, and E. K. Plyler, "Lines intensities of the CO_2 Σ-Σ bands in the 1.43-1.65 μ region," J. Mol. Spectrosc. **38**, 107–117 (1971).
[42]S. Hanf, R. Keiner, D. Yan, J. Popp, and T. Frosch, "Fiber-enhanced Raman multigas spectroscopy: A versatile tool for environmental gas sensing and breath analysis," Anal. Chem. **86**, 5278–5285 (2014).
[43]R. Šmíd, A. Hänsel, L. Pravdová, J. Sobota, O. Číp, and N. Bhattacharya, "Comb mode filtering silver mirror cavity for spectroscopic distance measurement," Rev. Sci. Instrum. **87**, 093107 (2016).